10

Handling of InGaAs quantum well parameters in the active region of near-IR LEDs (850−960 nm)

© R.A. Salii, A.V. Malevskaya, D.A. Malevskii, S.A. Mintairov, A.M. Nadtochiy, N.A. Kalyuzhnyy

Ioffe Institute,
St. Petersburg, Russia

e-mail: r.saliy@mail.ioffe.ru

Received May 03, 2024
Revised September 17, 2024
Accepted October 30, 2024

The flexible control of the radiation wavelength of $In_xGa_{1-x}As/Al_{0.3}Ga_{0.7}As$ multiple quantum wells for active area of near-IR LEDs (850−960 nm) has been experimentally demonstrated by changing their thickness and composition x. Heterostructures with multiple quantum wells demonstrating high photoluminescence intensity have been obtained using the MOVPE technique. Due to a unified post-growth technology of transferring heterostructures to a carrier-substrate and identical installation procedures, the manufactured LEDs demonstrated close electro-optical characteristics: efficiency from 50 to 54% and external quantum efficiency from 48 to 50%.

Keywords: quantum well, LED, InGaAs, MOVPE, heterostructures.

DOI: 10.61011/EOS.2024.11.60312.6568-24

Near-infrared (IR) light-emitting diodes (LEDs) are actively used in applications such as video surveillance, night vision systems, aerial drones, remote control, rangefinders for digital imaging, and time-of-flight sensors [1]. The use of multiple InGaAs/AlGaAs quantum wells (QWs) as the active region of such devices offers several advantages over conventional double heterostructures. In addition to providing enhanced electron-hole overlap, which leads to an increase in the radiative recombination rate and a significant improvement in the internal quantum yield, QWs also provide a high degree of control over the emission wavelength. Due to the quantization of energy in the QW it is possible to control its energy spectrum very precisely (with a small step in the emission wavelength of the active region). This technological and constructive possibility for the creation of IR emitters is investigated and illustrated in this study.

Based on the solid-state model [2], the thicknesses and composition of QWs were calculated $In_xGa_{1-x}As/Al_{0.3}Ga_{0.7}As$ for the near-IR wavelength range within 850−960 nm. Experimental heterostructures (HSs) of multiple QWs for the active area of LEDs emitting at wavelengths of 850, 870, 905, 910, 920, 940, and 960 nm were developed based on the calculation results. The investigated HSs were grown by metal-organic vapor phase epitaxy (MOVPE). The structures included wide-gap $Al_{0.3}Ga_{0.7}As$ barriers with thicknesses of 200 and 50 nm, between which there was an active area of five QWs. In order to generate radiation of the required wavelength, the thickness of the QWs (from 30 to 75 Å) and the In concentration (from 11 to 19%) were varied. In addition, the technology of embedding layers compensating elastic stresses in the active area was applied for all experimental HS. Multiple QWs introduce mechanical stresses into the semiconductor matrix associated with the mismatch of crystal lattice parameters, which leads to defect formation and, consequently, to limitations on the LED power output [3]. In [4–6], it was shown that the use of multiple quantum wells (MQWs) in the active area to compensate for mismatch-induced stresses significantly improves the performance of such LEDs. In this paper, depending on the In concentration and the thickness of the QW, $Al_xGa_{1-x}As_yP_{1-y}$ or $GaAs_xP_{1-x}$ solid solutions were used as compensating layers.

In Fig. 1, *a* in the investigated range of thicknesses and In concentration, the solid lines show the results of the solid-state model calculation for $In_xGa_{1-x}As/Al_{0.3}Ga_{0.7}As$, QWs emitting in the 850−960 nm range. The symbols in the diagram indicate the thickness and composition combinations that were chosen for the experimental HSs and for which photoluminescence (PL) spectra were measured. The PL spectra were measured at two optical excitation densities with a DTL-413 solid-state laser emitting at a wavelength of 527 nm.

Experimental HSs with two combinations of the QW parameters were created: 1) the one with reduced In composition but increased thickness and 2) the one with thickness reduced due to increased In concentration. As a result, first of all, the overall high level of PL intensity was observed for all grown HSs regardless of the QW composition and thickness. Fig. 1, *b* shows the relative integrated PL intensity of the obtained HS normalized to the result of the sample emitting at a wavelength of 940 nm, in which the maximum (within the investigated range) In concentration (19%) was used. Some non-uniformity of the PL intensity at different wavelengths can be explained by the increased sensitivity to the parameters of the layers compensating mechanical stresses, the problems of optimizing which for each wavelength are separate engineering

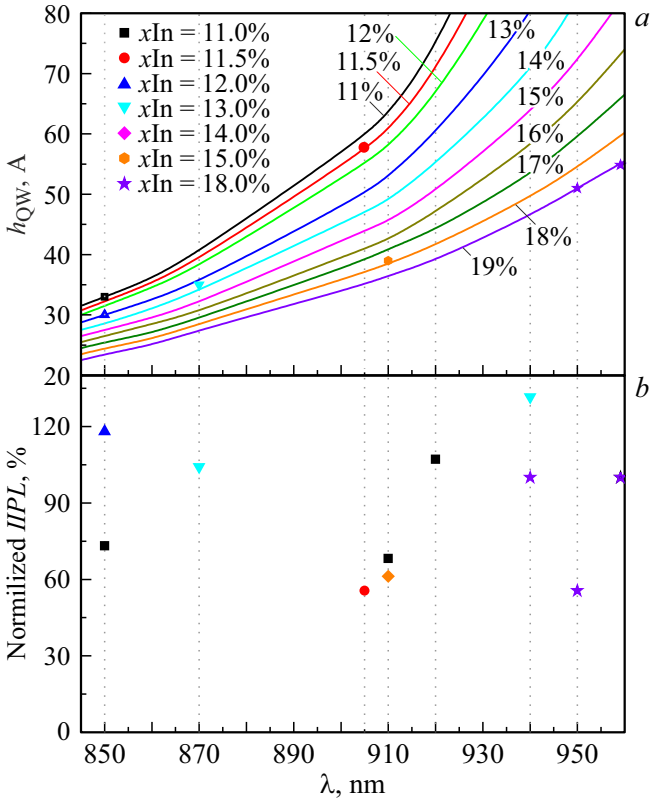

Figure 1. (*a*) Calculation results of the thickness (h_{QW}) and composition of the QWs $In_xGa_{1-x}As/Al_{0.3}Ga_{0.7}As$ for the wavelength range of 850–960 nm (solid lines — calculation, symbols — experimental data); (*b*) relative integral PL intensity (*IIPL*) of the obtained HSs with QW, normalized to the result of a sample with an emission wavelength of 940 nm, having In 19% concentration.

tasks that are beyond the scope of this study. Secondly, in accordance with the calculation performed, the possibility of flexible control of the wavelength with a step of 5–10 nm is shown. It is shown that the coupled variation of the In concentration in $In_xGa_{1-x}As$ and the thickness of the QW allows the optimal active region for LEDs to be determined experimentally. Based on the developed HS, LED structures were grown by MOVPE method, the sequence of layers in which is shown in general in Fig. 2.

Depending on the given wavelength, the active region containing the MQWs was modified according to the developed HSs. Several LED heterostructures emitting at wavelengths of 850, 910, and 940 nm (designated as 850LED, 910LED, and 940LED, respectively) were grown based on test structures whose active area had the maximum intensity of the PL peak. From the obtained LED heterostructures, devices were fabricated using a post-growth technique of transferring the HS onto a carrier substrate and sputtering the back reflector [7], texturing the light-emitting surface [8] and then installing a spherical optical element.

p-GaAs	Contact	
p-AlGaAs	Barrier/Stop-layer	
p-$Al_{0.3}Ga_{0.7}As$	Barrier	0.3 μm
	MQW active area	
n-$Al_{0.3}Ga_{0.7}As$	Barrier	0.3 μm
n-$Al_{0.2}Ga_{0.8}As$	Spreading layer	6 μm
n-GaAs	Contact	
AlGaAs	Sacrifice layer	
GaAs	Wafer	

Figure 2. Schematic representation of the LED structure in which the MQW active area was formed based on the study of the PL spectra of the HS for three wavelengths of the IR range: 850, 910, and 940 nm.

The sequence of operations of this technology conditionally includes 4 stages. At the first stage, point contacts are formed on the HS surface. Then by etching the *p*-GaAs contact layer is removed in places free from point contacts to form transparent windows for generated radiation. A dielectric coating is then deposited and a continuous backside metal reflector is formed on its surface, covered by additional protective barrier layers. In the second step, the HS is flipped and fixed on a carrier substrate (*n*-GaAs) with pre-deposited contact layers on its front and back surfaces. In the third step, the *n*-GaAs growth substrate is removed by selectively etching it down to the $Al_{0.9}Ga_{0.1}As$ stop layer, which also acts as a „sacrificial" layer and is then also etched down to the *n*-GaAs contact layer. In the fourth step, the light-emitting surface of the LED is textured, followed by the formation of a luminescent coating and sputtering of strip contacts to the *n*-GaAs layer. The main result of the post-growth procedure is the almost complete elimination of absorption losses in the structure for IR radiation of the investigated range (including absorption losses on free carriers), as well as the creation of an effective rear reflector for this radiation.

Fig. 3 shows the measured current dependences of energy efficiency (η), external quantum efficiency (EQE) and output optical power (P_{opt}) of the obtained LEDs. The measurements were performed using a reference photodetector with known spectral photosensitivity in a wide range of currents 0–1000 mA, passed through the investigated samples in pulsed mode. A pulsed current (5–300 μs less than 1%) was passed through the LED chip and the voltage was recorded. The generated LED radiation was absorbed by the control silicon photoconverter FDUK-100, whose spectral sensitivity in the wavelength range under study is 0.4 A/W. The flowing current was recorded, after which the optical power of the LED was calculated. To

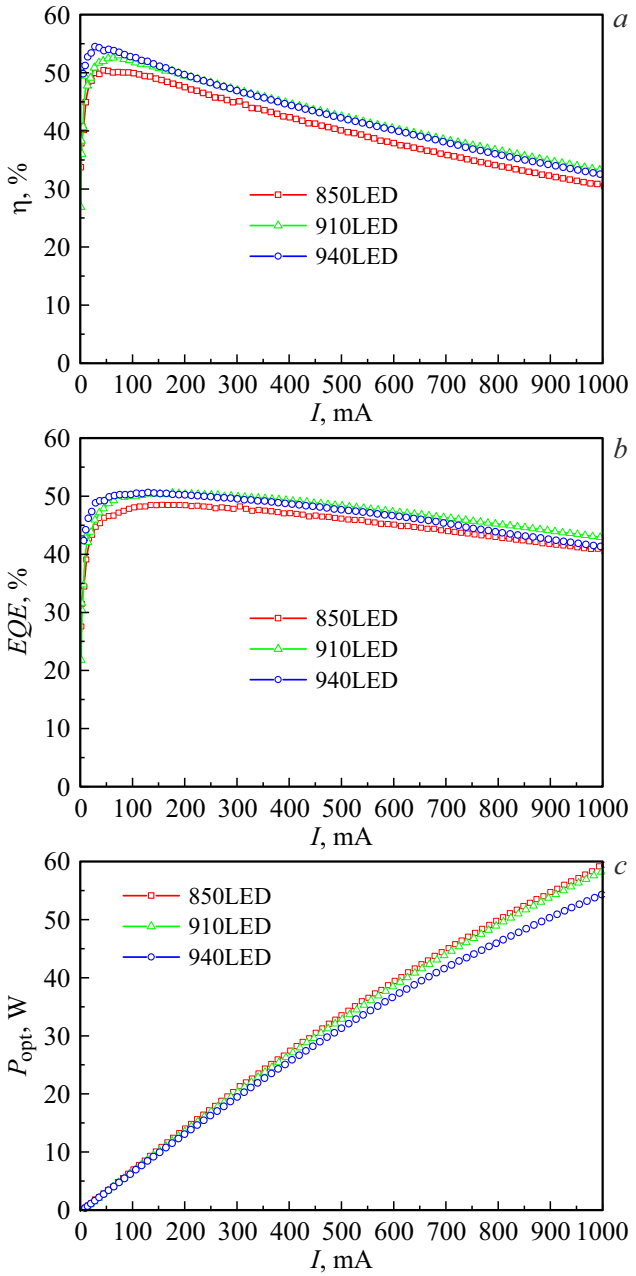

Figure 3. Current dependences: (*a*) energy efficiency, (*b*) external quantum efficiency, (*c*) output optical power of the obtained LEDs.

minimize the effect of angular divergence of radiation on the measurement results, the investigated samples and the control photodetector were placed in an integrating sphere with a light shield, which prevents the passage of direct radiation. A scattering coating was applied to the inner surfaces of the sphere and the screen. The spectral characteristics were measured in the sensitivity range of 300–1100 nm. EQE was determined using the measured current-power curves, and η was estimated as the ratio of the output optical power to the electrical power injected into the LED.

Due to the same post-growth technology and packaging technique, the LEDs (made based on the active area HS, which showed approximately the same PL intensity) also showed a correlated result when comparing the electro-optical characteristics. The η value for the obtained devices ranges from 50 to 54%, and EQE — from 48 to 50% (Fig. 3, *a, b*). It can be seen that at low currents, the value of η is higher than that of EQE. This result indicates low resistive losses in the devices. Indeed, the values of η and EQE are determined by the expressions

$$EQE = \frac{P/h\nu}{I/q}, \tag{1}$$

$$\eta = \frac{P}{IV}, \tag{2}$$

where P — the optical radiation power output from the LED, q — the electron charge, I — the injection current. The forward bias voltage of the LED (V) should in the limit be equal to the band gap or the energy of the light quanta (divided by q):

$$V = V_{\text{th}} = \frac{h\nu}{q} \approx E_g/q.$$

However, according to [9], due to the series resistance (R_s) of the diode (caused by resistance at the contacts, heterointerface of the structure, and so on), there is an additional voltage drop, so an increase in the excitation voltage is necessary to convert the energy of the injected electrons into the energy of a quantum of light:

$$V = V_{\text{th}} + IR_s.$$

Thus, at high R_s the energy efficiency will always be lower than the external quantum efficiency. However, the opposite is observed on the devices created, the value of V is less than V_{th}. This is due to the fact that, on the other hand, during the injection of hot carriers into the QW even before the full opening of the p–n- transition, part of the thermal energy is converted into light energy. Since in the investigated devices the value of η is greater than the value of EQE up to ~ 170 mA, we can conclude that there are no resistive losses in the heterostructure, as well as the high quality of metal/semiconductor contacts.

It should be noted that the EQE reduction effect, which is typical for this kind of devices [10], does not exceed 10% when the current reaches 1 A (Fig. 3, *b*). This indirectly indicates the low defect density in the MQW due to the use of the strain compensation technology. The value of the output optical power (P_{opt}) of all obtained LEDs increases sublinearly in the whole investigated current range (Fig. 3, *c*). Thus, for the 850LED sample, the P_{opt} was 70 mW at 100 mA and 590 mW at 1 A current; for the 910LED P_{opt} was 68 mW at 100 mA and 580 mW at 1 A current; for the 940LED P_{opt} was 66 mW at 100 mA and 550 mW at 1 A current.

Thus, in this work, the technological possibility of controlling the emission wavelength of MQW for the spectral range

850–960 nm by changing the QW parameters, which are part of the active area of the LED, has been experimentally shown. The investigated MQWs showed close PL intensity, which also indicates close values of the internal quantum yield (IQE) made based on them. The relationship between the values of IQE and measured EQE can be represented by the optical radiation output coefficient (K_{extr}), which is defined as the ratio of the number of photons emitted by the LED to the number of photons generated per unit time in the active area $EQE = IQE \cdot K_{\text{extr}}$. According to [9], it is virtually impossible to make K_{extr} greater than 50% without a sophisticated post-growth process. The K_{extr} parameter represents the quality of the light output, i.e., the manufacture of the device. In this study, the LEDs for $\lambda = 850$, 910, 940 nm wavelengths showed close EQE values (more than 50%). This indicates a well-established post-growth technology, including the technology of structure transfer to the carrier substrate, as well as the absence of additional photon absorption in the designed device structure for the entire spectral range 850–940 nm and the efficiency of the formed back reflector for this radiation.

Conflict of interest

The authors declare that they have no conflict of interest.

References

[1] M. Vasilopoulou, A. Fakharuddin, F. Pelayo García de Arquer, D.G. Georgiadou, H. Kim, A.R.M. Yusoff, F. Gao, M.K. Nazeeruddin, H.J. Bolink, E.H. Sargent. Nat. Photonics, **15**, 656–669 (2021). DOI: 10.1038/s41566-021-00855-2
[2] C.G. Van de Walle. Phys. Rev., **39** (3), 1871 (1989). DOI: 10.1103/PhysRevB.39.1871
[3] S.-D. Kim, H. Lee, J.S. Harris. J. Electrochem. Soc., **142** (5), 1667–1670 (1995). DOI: 10.1149/1.2048636
[4] Y. Yu, X. Qin, B. Huang, J. Weia, H. Zhou, J. Pan, W. Chen, Yun Qi, X. Zhang, Z. Ren. Vacuum, **69**, 489–493 (2003). DOI: 10.1016/S0042-207X(02)00560-2
[5] D.-K. Kim, H.-J. Lee. J. Nanosci. Nanotechnol., **18** (3), 2014–2017 (2018). DOI: 10.1166/jnn.2018.14952
[6] D.P. Xu, M.D. Souza, J.C. Shin, L.J. Mawst, D. Botez. J. Cryst. Growth, **310**, 2370–2376 (2008). DOI: 10.1016/j.jcrysgro.2007.11.218
[7] A.V. Malevskaya, N.A. Kalyuzhnyy, F.Y. Soldatenkov, R.V. Levin, R.A. Salii, D.A. Malevskii, P.V. Pokrovskii, V.R. Larionov, V.M. Andreev. Tech. Phys., **68** (1), 161–165 (2023). DOI: 10.21883/TP.2023.01.55451.166-22.
[8] A.V. Malevskaya, N.D. Il'inskaya, N.A. Kalyuzhnyy, D.A. Malevskiy, Yu.M. Zadiranov, P.V. Pokrovskiy, A.A. Blokhin, A.V. Andreeva. Semicond., **56** (13), 1086–1090 (2021). DOI: 10.21883/SC.2022.13.53906.9679.
[9] J. Cho, E.F. Schubert, J.K. Kim. Laser Photonics Rev., **7** (3), 408 (2013). DOI: 10.1002/lpor.201200025
[10] E.F. Shubert. *Light-Emitting Diodes,* second edition (Cambridge University Press, 2006). DOI: 10.1017/CBO9780511790546

Translated by J.Savelyeva